Determination of yield distribution in olefin production by thermal cracking of atmospheric gasoil

Sorood. Zahedi. Abghari[†], Jafar. Towfighi. Darian, Ramin. Karimzadeh, and Mohammad Reza Omidkhah

Chemical Engineering Department, Faculty of Engineering, Tarbiat Modares University, P.O. Box 14115-143, Tehran, Iran
(*Received 9 September 2007 • accepted 18 October 2007*)

Abstract−A pilot plant was designed and set up to study the thermal cracking of atmospheric gasoil. Based on the CCD (central composite design) method, a set of systematic experiments were designed and carried out. The designed variables were COT (coil outlet temperature), steam ratio and feed flow rate. The ranges of these variables were, respectively, equal to 716-884 °C, 0.46-1.136 and 0.977-6.02 g/min. The obtained minimum and maximum yield of ethylene was, respectively, equal to 1.7% and 30.9%, as well as the maximum yield of propylene was 12.2%. To predict the yield distribution of products and the coke formation in the range of operating conditions, a mechanistic model was developed based on experimental results. To analyze and characterize the atmospheric gasoil, a novel algorithm was applied. This algorithm utilized density, ASTM distillation curve, H/C ratio and the total aromatic fraction and generates the detail analysis of feedstock including paraffinic, naphthenic, aromatics and poly aromatic compounds.

Key words: Thermal Cracking, Atmospheric Gasoil, Feed Characterization, Modeling, Experimental Design

INTRODUCTION

Thermal cracking of hydrocarbons with steam is the main process for production of ethylene, propylene and other light olefins [1,2]. In this process, and in order to increase the olefin selectivity and decrease coke formation rate, feed is mixed with dilution water and introduced to a tubular reactor with high temperature and short residence time. The steam ratio value is varied and depends on consumed feedstock. While the range for ethane and propane is between 0.3 and 0.4, the range for naphtha would be 0.6 to 0.7. The diluted feed is preheated close to the cracking temperature depending on the hydrocarbon feed type.

Coke formation is always accompanied with pyrolysis of hydrocarbons. The coke deposits on the inner side of the reactor tube. The deposition not only affects the heat transfer but also increases the pressure drop of the fluid. It increases hot spot formation and would decrease the operating cycle and the capacity of the plant as well [3].

The homogeneous cracking reactions are endothermic; consequently, energy is required to elevate the gas temperature about 700-875 °C at the outlet of the reactor coils [4,5].

Common feedstocks for this unit are paraffinic hydrocarbons in the ranges between ethane to naphtha. The rise in naphtha prices and a growing demand for lighter hydrocarbons have caused the propensity of the higher boiling petroleum fractions as feedstock for olefin production. For this purpose, gasoils are the main choices.

Different aspects of thermal cracking of gasoils have been studied by different authors [6-12]. Zdonik et al. [6] introduced BMCI, molecular weight and hydrogen content as the vital parameters in characterizations of different gasoils as feed stocks of thermal cracking. Kaiser et al. [7] reported the yield distribution of thermal cracking of several feedstocks including ethane, propane, butanes, full range naphtha cuts and atmospheric gasoil. According to the research, the yield of ethylene production goes from 80 percent for ethane to 25 percent for gasoil. Hirato et al. [8] were the pioneers of proposing a model for thermal cracking of atmospheric gasoil. Some experiments were carried out and a molecular-based model was developed. Later, the proposed model was modified for modeling of thermal cracking of naphtha and kerosene [9]. Depeyre et al. [10] have performed some experiments and developed a model based on radical mechanism to predict the yield distribution of products. Conducted experiments had some limitations such as the steam ratio, as an operating parameter, has not been sufficiently varied in the designed experiments. Clymans et al. [11] collected extensive data on the thermal cracking of various fractions resulting from hydrotreatment of virgin vaccum gasoil. The fractions were hydrotreated naphtha, kerosene, atmospheric gasoil and vacuum gasoil. The potential of these fractions was evaluated as a feedstock for olefin production. Ranzi et al. [12,13] and Gwyn [14] have developed two different kinds of model to predict the thermal cracking of a wide variety of feed stocks including gasoils.

In addition, Shubo et al. [15] have studied the effects of coke inhibitors on coke formation rate and the yield of different products in thermal cracking of atmospheric gasoil. A kinetic mechanism for coke formation was introduced as well.

The scope of this paper is to study the product yield distribution of thermal cracking of atmospheric gasoil. Several experiments were carried out to study the effects of variation of different variables on the product yield distribution.

In order to generate systematic experimental data for covering a wide range of operating conditions, CCD as a systematic experimental design method was utilized. And based on the results, a semi mechanistic model was developed. In addition to the previous models, the new developed model determines the effects of all of the coke precursors as acetylene, olefins, aromatics and poly aromatics in coke formation.

[†]To whom correspondence should be addressed.
E-mail: sorood.zahedi@gmail.com

EXPERIMENTAL SECTIONS

1. Feed Characteristics

The selected atmospheric gasoil had boiling range of 218 °C to 387 °C with a density of 0.845 g/cm³. The main properties of this hydrocarbon feed are listed in Table 1. The BMCI and coking inhibi-

Table 1. The main properties of the atmospheric gasoil

Specification	Gas-oil
Sulfur, Total wt%	0.75
Nitrogen, Total wt%	<0.5
Hydrogen, Total wt%	13.8
Carbon, Total wt%	85.6
Aromatic Content, vol%	14
Olefin content, vol%	Trace<0.3
Saturate Content, vol%	86
Distillation:	°C
IBP at 760 mm Hg	218
5%Vol. Recovery	257
10%Vol. Recovery	266
30%Vol. Recovery	285
50%Vol. Recovery	303
70%Vol. Recovery	324
90%Vol. Recovery	362
FBP at 760 mm Hg	387

tion index of the selected atmospheric gasoil are, respectively, 28.26 and 36.75 [16], showing low enough coking intensity for the selected atmospheric gasoils [10,15].

2. Pilot Plant Setup

The experiments were performed in a pilot setup that was designed and assembled for thermal cracking of the hydrocarbon feed stocks in the range from ethane to gasoils. This pilot can be fed either by liquid or gas hydrocarbons. Liquid hydrocarbons and dilution water were fed through dosing pumps. However, gas hydrocarbons were fed to the pilot through a regulator and a mass flow meter. The feed flow rates and steam ratio respectively varied from 1 to 15 g/min and 0.3 to 1.0 (Fig. 1).

The hydrocarbon and dilution water were heated up to the cracking temperature (550 °C) by two separated furnaces. The transfer lines from dosing pumps to preheaters were isolated and heated to 200 °C by a heater-isolator. The reactor furnace has been divided into three zones, which can be heated independently to control the temperature profile. The reactor has 1 m length, 12 mm internal diameter and it is made of Inconel 600. There are twelve thermocouples along the reactor: six inside the furnace, four on the tube skin and two additional thermocouples for measuring of the XOT (cross-over temperature) and COT.

The reactor effluent is immediately quenched by cooling water in a double pipe heat exchanger. In order to separate the condensate from gaseous product stream, the exchanger outlet stream is sent to a flash drum then the gas phase passes through a series of condensers and is entered in a filter in the final stage.
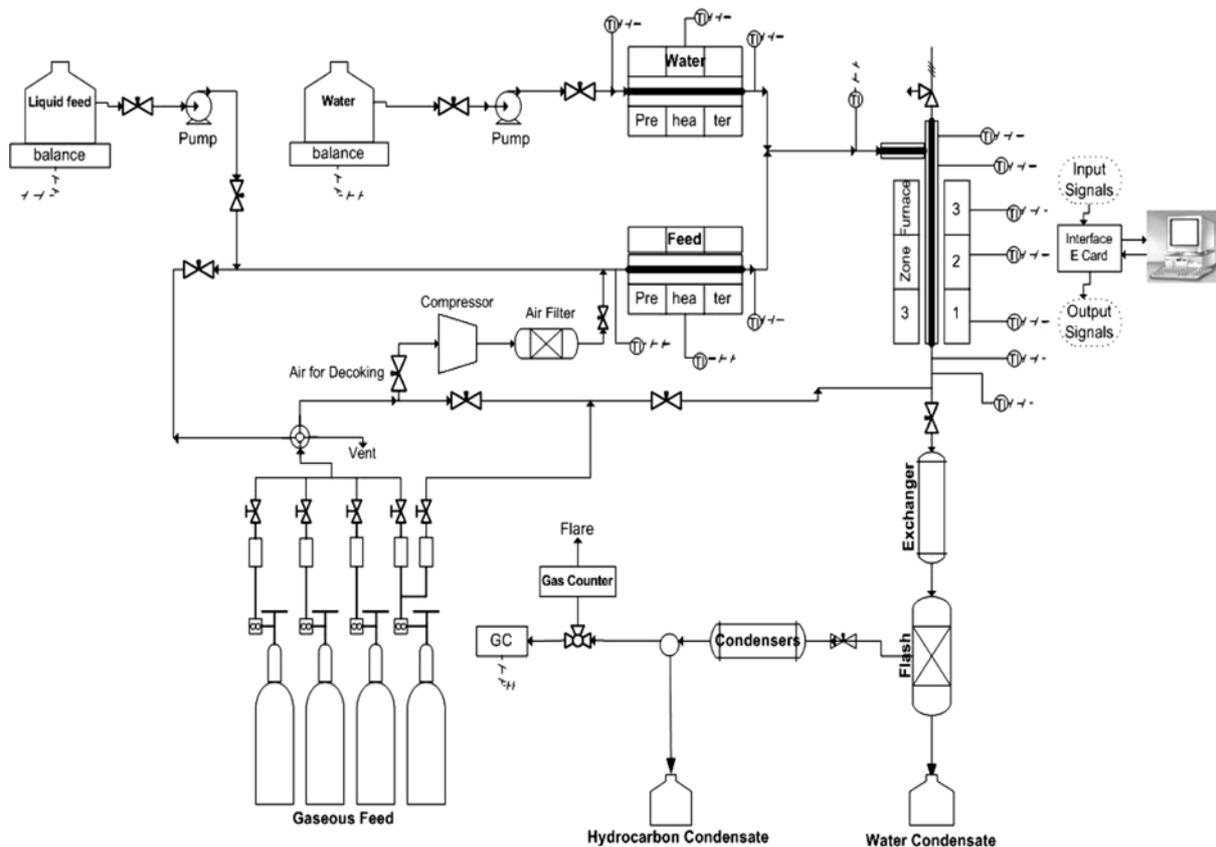

Fig. 1. Schematic diagram of the thermal cracking pilot plant setup.

Table 2. Calculated analysis (molar fraction) of atmospheric gasoil

	Paraffins		Naphthenes		Aromatics		Total
	Normal	Iso	Mono	di	Alkyl	Poly	
C9	0.002608	0	0.0059928	0	0.006322	0	0.014923
C10	0.031167	0.0010865	1.33E-05	0.04317	0.02015	0	0.095587
C11	0	0.052248	0.011487	0	0.026889	0	0.090624
C12	0.00073	0.012663	0.0038285	0.005584	0.006807	0	0.029612
C13	0.031805	0	0.067761	0.012622	0	0	0.112188
C14	0.051306	0	0	0	0.002663	0	0.053969
C15	0	0.065233	0.047358	0	0.003703	0	0.116294
C16	0	0.018596	0	0	0.008816	0	0.027412
C17	0.041701	0.014984	3.43E-02	0	0	0	0.091024
C18	0.044747	0.021968	0.034659	0	0	0	0.101374
C19	0	0.017358	0.0090544	0	0.022495	0.005446	0.054353
C20	0.024946	0.014035	0.00095784	0	0.019009	0.0229	0.081848
C21	0.054244	0	0.018697	0	0	0	0.072941
C22	0.007445	0	0.012488	0	0	0	0.019933
C23	0.023865	0.0090854	0	0	0	0	0.03295
C24	0.004978	0	0	0	0	0	0.004978
C25	0	0	0	0	0	0	0
	0.319542	0.2272569	0.24663585	0.061376	0.116854	0.028346	1.00001

After each run, a fraction of product gas is withdrawn for analysis by a Varian Chrompack CP3800 gas chromatograph.

MATHEMATICAL MODELING

1. Feed Characterization Model

The characterization of feedstock is a vital step in modeling and kinetic analysis of refineries and petrochemical processes. In fact, the interaction effects of different feed species on product yield distributions are concerned as the main reasons. The problem becomes more crucial when the heavy feedstocks, containing hydrocarbons with more than 10 carbons, are used. In this case, the existence of several hydrocarbons with almost the same physical properties makes the detail analysis complicated and even unattainable. In order to tackle the problem, several researches have been carried out [14,17] to improve analysis methods or to produce some useful library data. However, in some cases, the available data is limited; thus detailed analysis is more convincing with the help of some correlations. In fact, these correlations were derived to estimate properties of different cuts in a complex hydrocarbon feeds.

Gwyn [14] applied these correlations and used RI (Refractive Index), density and TBP (True Boiling Points) curve to identify the PNA (Paraffins, Naphthenes and Aromatics) analysis of thermal cracking feed stock. Taskar et al. [18] developed an algorithm and used ASTM distillation curve and density to estimate heavy naphtha detail analysis. Zahedi et al. [19] used the algorithm and estimate the naphtha analysis with 26 pseudo components as a feedstock for catalytic reformers.

In this work the density, ASTM distillation curve, H/C ratio and total aromatic fraction were used to determine the detailed analysis of atmospheric gasoil. The major steps in the feed characterization algorithm are listed below [18]:

1. ASTM distillation curve is converted to TBP by defined relations.

2. Englar slope, mean average boiling point and Watson K-factor are calculated by empirical relations.

3. The specific gravity of each volume fraction is calculated concerning the specific gravity of the mixture and Watson K-factor.

4. The molecular weight of each fraction is composed of the molecular weights of the components constituting that fraction [20]. In order to determine the quantity of chemical species in a fraction and mixture, a nonlinear optimization search is applied. Nevertheless, adding more equations is useful to increase the accuracy of the optimization procedure. H/C ratio and total volume fraction is valuable information in this case.

The defined optimization problem is accompanied with some constraints. First, the molar fraction of each composition must be between 0 and 1. Then the summation of molar fractions is also equal to 1.

Table 2 shows the calculated analysis for atmospheric gasoil. The analysis contains n-paraffins, iso-paraffins, mono and di-cyclic naphthenes, alkyl aromatics and poly aromatics species.

2. Reactor Model

The one-dimensional plug flow reactor hypothesis is applied to modeling and simulating of the reactor of thermal cracking pilot plant. This is a non isothermal and non adiabatic reactor.

The modeling and simulating requires the integration of a set of continuity equations for the process gas species, together with the energy and momentum balance equations as follows:

Mass balance:

$$\frac{dF_i}{dz} = \left(\sum_i S_{ij} r_{ri}\right) \frac{\pi d_t^2}{4} \quad (1)$$

Energy balance:

$$\sum_j F_j C_{Pj} \frac{dT}{dz} = Q(z) \pi d + \frac{\pi d_t^2}{4} \sum_i r_{ri} (-\Delta H)_i \quad (2)$$

Momentum balance:

$$\frac{dP}{dz} = \frac{\frac{d}{dz}\left(\frac{1}{M_m}\right) + \frac{1}{M_m}\left(\frac{1}{T} \cdot \frac{dT}{dz} + Fr\right)}{\frac{1}{M_m P} - \frac{P}{aRTG^2}} \qquad (3)$$

Fr is the friction factor and calculated by the following equation:

$$Fr = 0.092\frac{Re^{-0.2}}{d_t} \qquad (4)$$

3. Kinetic Modeling

Free radical chain mechanism is widely accepted for thermal cracking reactions [10,12,13,15,21]. For thermal cracking of atmospheric gasoil a kinetic model, based on the literature, was developed [10, 22,23]. The developed model predicts all light products including acetylene, olefins and light paraffins. It also determines the yield of alkyl aromatics as benzene, toluene, ethylbenzene and xylenes. Furthermore, to describe the contribution of olefins [15], acetylene and aromatics in coke formation, the kinetic model utilizes some reactions. In the proposed reaction network, the alkyl aromatics and poly aromatics species of feedstock were only contributed in coke formation. The reaction network is listed in Table 6.

To avoid complexity in reaction network, the detected species of atmospheric gasoil (Table 2) were lumped to five pseudo components as n-$C_{16}H_{34}$ and i-$C_{16}H_{34}$ for normal paraffins and iso paraffins, $C_{13}H_{26}$ for naphthenes, $C_{15}H_{34}$ for alkyl-aromatics and $C_{20}H_{28}$ for poly aromatics. The reaction network was designed based on these pseudo components.

The experiments conducted for the determination of kinetic parameters were carried out at atmospheric pressure with the coil out-

let temperature in the range of 716-884 °C. The dilution steam ratio was in the range of 0.46-1.14 and feed flow rate was varied from 0.977 g/min to 6.02 g/min.

CCD method [24] was applied with three design factors, namely, the hydrocarbon feed flow rate (X1), the steam ratio (X2) and coil outlet temperature (X3). The coded levels and the natural values of the factors are shown in Table 3.

Eleven response variables have been concerned including product yield of the main primary products and the rate of coke formation. The number of trials was based on the number of the design factors and was equal to 19 experiments (15 combinations with four replications). Results of the experiments and the design matrix are shown in Table 4. Production yields of light olefins as ethylene, propylene, butadiene and butenes and production yield of light paraffins as methane, ethane, propane and rate of coke formation were taken as response variables.

The governing mass, energy, and momentum balance equations for the reactor tube constitute a boundary value problem which is highly stiff in numerical simulation due to the large differences in concentration gradient between radicals and molecules. This problem can be resolved with modified Euler or Gear method [25].

In order to determine the kinetic parameters, the residual sum of

Table 5. Yield of BTEX during thermal cracking of atmospheric gasoil at different operating conditions

	Test-1	Test-2	Test-3	Test-4	Test-5
COT (°C)	754.8	853	794.5	802	825
Feed flow rate (g/min)	4.91	4.98	6.03	3.26	4.92
Steam ratio	0.613	0.97	0.755	0.904	0.955
Residence time (sec)	0.296	0.237	0.23	0.376	0.247
Yield of BTEX					
Benzene (mass %)	0.859	1.444	0.636	0.816	0.877
Toluene (mass %)	0.76	1.404	0.609	0.958	0.800
Ethylbenzene (mass %)	0.35	0.237	0.214	0.381	0.330
Xylenes (mass %)	0.22	0.755	0.187	0.323	0.423

Table 3. Coded and natural levels of the design factors

Design factors	−1.6818	−1	0	1	1.6818
X1:feed flow rate	0.977	2	3.5	5	6.02
X2:Steam ratio	0.46364	0.6	0.8	1.0	1.13636
X3:Coil outlet temperature	716	750	800	850	884

Table 4. Design matrix and results of the central composite design

NO	1	2	3	4	5	6	7	8	9	10	11	12	13	14	15	16	17	18	19
X1	−1	−1	−1	−1	1	1	1	1	−1.68	1.68	0	0	0	0	0	0	0	-1	-1
X2	−1	−1	1	1	−1	−1	1	1	0	0	-1.68	1.68	0	0	0	0	0	1	1
X3	−1	1	−1	1	−1	1	−1	1	0	0	0	0	-1.68	1.68	0	0	0	1	1
Y1 (C_2H_4)	11.6	26.5	10.2	26.9	7.9	26.7	2.1	20.8	17.8	9.58	21.4	15.1	1.7	30.8	18.4	17.7	17.2	26.6	26.5
Y2 (C_3H_6)	7.9	11.6	6.63	12.2	3.39	12.2	1.37	10.2	10.02	7.3	9.8	9.56	0.26	10.7	9.59	8.79	9.74	11.3	10.66
Y3 (CH_4)	3.7	9.8	3.1	8.99	1.39	8.83	0.58	5.55	7.5	4.6	9	3.79	2.24	10.7	5.13	5	4.74	9.02	8.96
Y4 (C_3H_8)	0.36	0.4	6.63	0.4	0.18	0.44	0.08	0.37	0.4	0.33	0.48	0.43	0.35	0.35	0.39	0.35	0.38	0.38	0.34
Y5 (C_2H_6)	1.7	2.3	1.34	2.04	1.04	2.5	0.27	1.52	2.11	1.56	2.54	1.33	1.31	2	1.85	1.71	1.66	2.07	2
Y6 (C_2H_2)	1.02	0.86	1.21	1.21	0.43	1.27	0.21	0.63	0.74	1.04	0.88	1.98	0.41	1.15	1.98	1.36	1.32	0.96	0.98
Y7 (C_4H_6)	1.62	5.65	1.68	4.8	1.05	3.6	0.52	3.05	2.51	0.33	3.61	2.4	1.37	7.1	2.11	2.24	2.1	4.93	5.03
Y8 (C_4H_8)	1.85	2.5	2.07	2.8	1.6	2.31	0.24	0.17	1.81	0.6	3.82	2.73	1.35	2.67	2.05	1.77	1.61	2.42	3.16
Y9 (H_2)	0.6	1.4	1.6	0.72	0.27	0.92	0.11	0.6	3.9	0.5	4.6	1.58	0.23	1.3	0.54	0.45	0.48	1.04	0.81
Y10 (C5+)	69.4	36.4	65.5	38.3	81.2	41.1	94.2	53.3	53.2	65.7	43.44	58.6	88.32	32.2	57.9	60.4	60.3	32.1	33.4
Rate of coke (gr/cm²·sec)*10⁷	1.67	34.1	0.66	20.9	0.16	18.2	0.03	3.9	12.3	0.51	11.53	0.65	0.06	32.4	1.6	2.35	2.4	24.6	25.6

Table 6. Reaction scheme for Thermal Cracking of Atmospheric gasoil

Number	Reaction	Parameters adopted	
		A	E
	1. Paraffin⇒Radical+Radical		
1	$C_{16}H_{34} \rightarrow C_8H_{17}^0 + C_8H_{17}^0$	1.44×10^{14}	250.92
2	$C_{16}H_{34} \rightarrow C_9H_{19}^0 + C_7H_{15}^0$	1.44×10^{14}	250.92
3	$C_{16}H_{34} \rightarrow C_{10}H_{21}^0 + C_6H_{13}^0$	1.44×10^{14}	250.92
4	$C_{16}H_{34} \rightarrow C_{11}H_{23}^0 + C_5H_{11}^0$	1.44×10^{14}	250.92
5	$C_{16}H_{34} \rightarrow C_{12}H_{25}^0 + C_4H_9^0$	1.44×10^{14}	250.92
6	$C_{16}H_{34} \rightarrow C_{13}H_{27}^0 + I - C_3H_7^0$	1.44×10^{14}	250.92
7	$C_{16}H_{34} \rightarrow C_{14}H_{29}^0 + C_2H_5^0$	1.44×10^{14}	250.92
8	$C_{16}H_{34} \rightarrow C_{15}H_{31}^0 + CH_3^0$	1.44×10^{14}	250.92
9	$C_{16}H_{34} \rightarrow C_{16}H_{33}^0 + H^0$	1.44×10^{14}	334.56
10	$i - C_{16}H_{34} \rightarrow C_{13}H_{27}^0 + 2 - C_3H_7^0$	1.44×10^{14}	250.92
11	$i - C_{16}H_{34} \rightarrow C_{15}H_{31}^0 + CH_3^0$	1.44×10^{14}	234.192
12	$C_{13}H_{26} \rightarrow 1 - C_6H_{11}^0 + C_7H_{15}^0$	1.4×10^{13}	255.102
	2. Radical⇒Olefin+Radical		
13	$C_{16}H_{33}^0 \rightarrow C_2H_4 + C_{14}H_{29}^0$	4×10^{14}	104.55
14	$C_{16}H_{33}^0 \rightarrow C_3H_6 + C_{13}H_{27}^0$	1.2×10^{14}	108.732
15	$C_{16}H_{33}^0 \rightarrow C_4H_8 + C_{12}H_{25}^0$	0.6×10^{13}	108.732
16	$C_{16}H_{33}^0 \rightarrow C_5H_{10} + C_{11}H_{23}^0$	0.6×10^{13}	125.46
17	$C_{15}H_{31}^0 \rightarrow C_2H_4 + C_{13}H_{27}^0$	4×10^{14}	104.55
18	$C_{15}H_{31}^0 \rightarrow C_3H_6 + C_{12}H_{25}^0$	1.2×10^{14}	108.732
19	$C_{15}H_{31}^0 \rightarrow C_4H_8 + C_{11}H_{23}^0$	0.6×10^{13}	108.732
20	$C_{15}H_{31}^0 \rightarrow C_5H_{10} + C_{10}H_{21}^0$	0.6×10^{13}	125.46
21	$C_{14}H_{29}^0 \rightarrow C_2H_4 + C_{12}H_{25}^0$	4×10^{14}	104.55
22	$C_{14}H_{29}^0 \rightarrow C_3H_6 + C_{11}H_{23}^0$	1.2×10^{14}	112.0776
23	$C_{14}H_{29}^0 \rightarrow C_4H_8 + C_{10}H_{21}^0$	0.6×10^{13}	112.0776
24	$C_{14}H_{29}^0 \rightarrow C_4H_8 + C_9H_{19}^0$	0.6×10^{13}	125.46
25	$C_{13}H_{27}^0 \rightarrow C_2H_4 + C_{11}H_{23}^0$	4×10^{14}	104.55
26	$C_{13}H_{27}^0 \rightarrow C_3H_6 + C_{10}H_{21}^0$	1.2×10^{14}	108.732
27	$C_{13}H_{27}^0 \rightarrow C_4H_8 + C_9H_{19}^0$	0.85×10^{13}	108.732
28	$C_{13}H_{27}^0 \rightarrow C_5H_{10} + C_8H_{17}^0$	0.85×10^{13}	125.46
29	$C_{12}H_{25}^0 \rightarrow C_2H_4 + C_{10}H_{21}^0$	4×10^{14}	104.55
30	$C_{12}H_{25}^0 \rightarrow C_3H_6 + C_9H_{19}^0$	1.2×10^{14}	108.732
31	$C_{12}H_{25}^0 \rightarrow C_4H_8 + C_8H_{17}^0$	0.6×10^{13}	108.732
32	$C_{12}H_{25}^0 \rightarrow C_5H_{10} + C_7H_{15}^0$	0.6×10^{13}	125.46
33	$C_{11}H_{23}^0 \rightarrow C_2H_4 + C_9H_{19}^0$	4×10^{14}	104.55
34	$C_{11}H_{23}^0 \rightarrow C_3H_6 + C_8H_{17}^0$	1.2×10^{14}	108.732
35	$C_{11}H_{23}^0 \rightarrow C_4H_8 + C_7H_{15}^0$	0.6×10^{13}	108.732
36	$C_{11}H_{23}^0 \rightarrow C_5H_{10} + C_6H_{13}^0$	0.6×10^{13}	125.46
37	$C_{10}H_{21}^0 \rightarrow C_2H_4 + C_8H_{17}^0$	4×10^{14}	104.55
38	$C_{10}H_{21}^0 \rightarrow C_3H_6 + C_7H_{15}^0$	1.2×10^{14}	108.732
39	$C_{10}H_{21}^0 \rightarrow C_4H_8 + C_6H_{13}^0$	0.6×10^{13}	108.732
40	$C_{10}H_{21}^0 \rightarrow C_5H_{10} + C_5H_{11}^0$	0.6×10^{13}	125.46
41	$C_9H_{19}^0 \rightarrow C_2H_4 + C_7H_{15}^0$	1×10^{15}	104.55
42	$C_9H_{19}^0 \rightarrow C_3H_6 + C_6H_{13}^0$	3.2×10^{14}	108.732
43	$C_9H_{19}^0 \rightarrow C_4H_8 + C_5H_{11}^0$	0.5×10^{14}	108.732
44	$C_9H_{19}^0 \rightarrow C_5H_{10} + C_4H_9^0$	1.01×10^{13}	138.006
45	$C_8H_{17}^0 \rightarrow C_2H_4 + C_6H_{13}^0$	1×10^{15}	121.278
46	$C_8H_{17}^0 \rightarrow C_3H_6 + C_5H_{11}^0$	3.2×10^{14}	117.096
47	$C_8H_{17}^0 \rightarrow C_4H_8 + C_4H_9^0$	5.66×10^{13}	121.278
48	$C_8H_{17}^0 \rightarrow C_5H_{10} + 1 - C_3H_7^0$	1.01×10^{13}	117.096

Table 6. Continued

Number	Reaction	Parameters adopted	
		A	E
49	$C_7H_{15}^0 \rightarrow C_2H_4 + C_5H_{11}^0$	1.18×10^{15}	121.278
50	$C_7H_{15}^0 \rightarrow C_3H_6 + C_4H_9^0$	3.2×10^{14}	117.096
51	$C_7H_{15}^0 \rightarrow C_4H_8 + 1 - C_3H_7^0$	5.66×10^{13}	121.278
52	$C_7H_{15}^0 \rightarrow C_5H_{10} + C_2H_5^0$	1.01×10^{13}	117.096
53	$C_6H_{13}^0 \rightarrow C_2H_4 + C_4H_9^0$	2.5×10^{13}	121.278
54	$C_6H_{13}^0 \rightarrow C_3H_6 + 1 - C_3H_7^0$	1.5×10^{13}	118.3506
55	$C_6H_{13}^0 \rightarrow C_4H_8 + C_2H_5^0$	5.66×10^{13}	121.278
56	$C_6H_{13}^0 \rightarrow C_5H_{10} + CH_3^0$	8.21×10^{13}	138.006
57	$1 - C_6H_{11}^0 \rightarrow 2 - C_6H_{11}^0$	0.72×10^{13}	0
58	$2 - C_6H_{11}^0 \rightarrow 1 - C_6H_{11}^0$	1.0×10^{14}	125.46
59	$1 - C_6H_{11}^0 \rightarrow C_2H_4 + C_4H_7^0$	1.056×10^{14}	125.46
60	$C_5H_{11}^0 \rightarrow C_2H_4 + 1 - C_3H_7^0$	3.95×10^{12}	121.278
61	$C_5H_{11}^0 \rightarrow C_3H_6 + C_2H_5^0$	5.0×10^{12}	121.278
62	$C_5H_{11}^0 \rightarrow C_4H_8 + CH_3^0$	3.2×10^{13}	131.733
63	$C_5H_{11}^0 \rightarrow C_5H_{10} + H^0$	5.0×10^{13}	153.0612
64	$C_4H_9^0 \rightarrow C_2H_4 + C_2H_5^0$	1.62×10^{12}	117.096
65	$C_4H_9^0 \rightarrow C_3H_6 + CH_3^0$	2.5×10^{12}	133.824
66	$C_4H_9^0 \rightarrow C_4H_8 + H^0$	2.0×10^{13}	167.28
67	$2 - C_3H_7^0 \rightarrow C_3H_6 + H^0$	2.0×10^{13}	163.098
68	$1 - C_3H_7^0 \rightarrow C_2H_4 + CH_3^0$	4.0×10^{13}	138.006
69	$1 - C_3H_7^0 \rightarrow C_3H_6 + H^0$	2.0×10^{13}	158.916
70	$C_2H_5^0 \rightarrow C_2H_4 + H^0$	3.2×10^9	167.28
71	$C_4H_7^0 \rightarrow C_4H_6 + H^0$	1.32×10^{14}	204.918
	3. Paraffin+Radical=>Paraffin+Radical		
72	$C_{16}H_{34} + H^0 \rightarrow C_{16}H_{33}^0 + H_2$	0.56×10^{11}	41.82
73	$C_{16}H_{34} + H^0 \rightarrow C_{16}H_{33}^0 + H_2$	4.6×10^{11}	34.7106
74	$C_{16}H_{34} + C_2H_5^0 \rightarrow C_{16}H_{33}^0 + C_2H_6$	4.6×10^{11}	29.274
75	$C_{16}H_{34} + 1 - C_3H_7^0 \rightarrow C_{16}H_{33}^0 + C_3H_8$	0.56×10^{11}	33.456
76	$1 - C_{16}H_{34} + H^0 \rightarrow 1 - C_{16}H_{33}^0 + H_2$	0.56×10^{11}	25.092
77	$1 - C_{16}H_{34} + CH^0 \rightarrow 1 - C_{16}H_{33}^0 + CH_4$	4.6×10^{11}	17.982
78	$1 - C_{16}H_{34} + C_2H_5^0 \rightarrow 1 - C_{16}H_{33}^0 + C_2H_6$	4.6×10^{11}	12.546
79	$1 - C_{16}H_{34} + C_2H_7^0 \rightarrow 1 - C_{16}H_{33}^0 + C_2H_8$	0.56×10^{11}	16.728
80	$C_3H_8 + H^0 \rightarrow 1 - C_3H_7^0 + H_2$	0.85×10^2	35.128
81	$C_3H_8 + CH_3^0 \rightarrow 1 - C_3H_7^0 + CH_4$	0.582×10^4	34.29
82	$C_3H_8 + 1 - C_3H_7^0 \rightarrow 1 - C_3H_7^0 + C_2H_6$	0.621×10^2	41.82
83	$C_2H_6 + H^0 \rightarrow C_2H_5^0 + H_2$	1×10^{11}	40.5654
84	$C_2H_6 + CH_3^0 \rightarrow C_2H_5^0 + CH_4$	3.8×10^{11}	69.003
85	$C_2H_6 + 1 - C_3H_7^0 \rightarrow C_2H_5^0 + C_3H_8$	0.3×10^7	50.184
86	$CH_4 + H^0 \rightarrow CH_3^0 + H_2$	0.62×10^4	50.184
87	$CH_4 + C_2H_5^0 \rightarrow CH_3^0 + C_2H_6$	0.32×10^7	75.276
88	$CH_4 + 1 - C_3H_7^0 \rightarrow CH_3^0 + C_3H_8$	0.78×10^7	79.458
89	$H_2 + CH_3^0 \rightarrow H^0 + CH_4$	0.14×10^{15}	50.184
90	$H_2 + C_2H_5^0 \rightarrow H^0 + C_2H_6$	0.80×10^{13}	58.548
91	$H_2 + 1 - C_3H_7^0 \rightarrow H^0 + C_3H_8$	0.32×10^{15}	50.184
	4. Radical+Radical=>Paraffin		
92	$1 - C_3H_7^0 + H^0 \rightarrow C_3H_8$	0.62×10^{14}	0
93	$C_2H_5^0 + H^0 \rightarrow C_2H_6$	4×10^4	0
94	$C_2H_5^0 + CH_3^0 \rightarrow C_3H_8$	0.3×10^{13}	0
95	$CH_3^0 + CH^0 \rightarrow C_2H_6$	1.30×10^{13}	0
96	$CH_3^0 + H^0 \rightarrow CH_4$	1×10^{24}	0

Table 6. Continued

Number	Reaction	Parameters adopted	
		A	E
97	$C_2H_3^0 + H^0 \rightarrow C_2H_4$	1.0×10^{11}	0
98	$C_2H_3^0 + H^0 \rightarrow C_2H_4$	2.00×10^{11}	0
99	$C_2H_3^0 + C_2H_3^0 \rightarrow C_4H_6$	1.00×10^{13}	0
100	$2 - C_3H_7^0 + H^0 \rightarrow C_3H_8$	0.13×10^{11}	0
	5. Secondary Reaction I: Olefin+Radical<=>Paraffin+Olefin Radical		
101	$C_3H_6 + H^0 \rightarrow C_3H_5^0 + H_2$	2.5×10^9	4.6
102	$C_3H_6 + CH_3^0 \rightarrow C_3H_5^0 + CH_4$	2.0×10^6	51.02
103	$C_3H_6 + C_2H_5 \rightarrow C_3H_5^0 + C_2H_6$	1.0×10^5	60.64
104	$C_3H_5^0 + C_3H_8 \rightarrow C_3H_6 + 1 - C_3H_7^0$	5.0×10^9	66.91
105	$C_4H_8 + H^0 \rightarrow C_4H_7^0 + H_2$	1.2×10^{12}	16.31
106	$C_4H_8 + CH_3^0 \rightarrow C_4H_7^0 + CH_4$	1.03×10^{13}	30.53
107	$C_4H_8 + C_2H_5^0 \rightarrow C_4H_7^0 + C_2H_6$	1.0×10^{13}	34.71
108	$C_4H_7^0 + C_3H_8 \rightarrow C_4H_8 + 1 - C_3H_7^0$	5.0×10^4	66.91
109	$C_5H_{10} + H^0 \rightarrow C_5H_9^0 + H_2$	5.0×10^9	16.728
110	$C_5H_{10} + CH_3^0 \rightarrow C_5H_9^0 + CH_4$	1.0×10^{13}	33.456
111	$C_5H_{10} + C_2H_5^0 \rightarrow C_5H_9^0 + C_2H_6$	5.0×10^{13}	33.456
112	$C_5H_9^0 + C_3H_8 \rightarrow C_5H_{10} + 1 - C_3H_7^0$	5.0×10^9	66.91
	6. Secondary Reaction II:		
113	$C_2H_4 + H^0 \rightarrow C_2H_3^0 + H_2$	0.8×10^7	16.728
114	$C_2H_4 + CH_3^0 \rightarrow C_2H_3^0 + CH_4$	0.1×10^9	54.366
115	$C_2H_4 + C_2H_5^0 \rightarrow C_2H_3^0 + C_2H_6$	3.0×10^7	79.46
116	$C_2H_4 + H^0 \rightarrow C_2H_5^0$	0.1×10^8	6.273
117	$C_2H_4 + CH_3^0 \rightarrow 1 - C_3H_7^0$	0.2×10^7	33.038
118	$C_2H_4 + C_2H_5^0 \rightarrow C_4H_9^0$	0.15×10^6	31.78
119	$C_2H_4 + C_2H_3^0 \rightarrow C_4H_6 + H^0$	0.12×10^{12}	204.92
120	$C_2H_4 + C_2H_3^0 \rightarrow C_4H_7^0$	6.078×10^7	29.274
121	$C_3H_6 + H^0 \rightarrow 1 - C_3H_7^0$	1.015×10^8	6.273
122	$C_3H_6 + C_2H_3^0 \rightarrow 1 - C_3H_7^0$	0.32×10^9	30.94
123	$C_4H_8 + H^0 \rightarrow C_4H_9^0$	0.48×10^9	31.36
124	$C_4H_8 + CH_3^0 \rightarrow C_3H_{11}^0$	0.112×10^{10}	30.11
	7. Molecular Reaction I:		
125	$C_3H_6 \rightarrow C_2H_2 + CH_4$	3.794×10^{11}	59.38
126	$C_2H_2 + C_2H_4 \rightarrow C_4H_6$	1.026×10^7	41.26
127	$C_4H_8 \rightarrow C_4H_6 + H_2$	8.385×10^8	200.99
128	$C_4H_6 + C_2H_4 \rightarrow C_6H_6 + 2H_2$	9.74×10^8	146.37
129	$C_4H_6 + C_3H_6 \rightarrow C_7H_8 + 2H_2$	6.4×10^{14}	150.552
130	$C_4H_6 + C_4H_8 \rightarrow C_8H_{10} + 2H_2$	1.51×10^8	245.7
131	$C_4H_6 + C_4H_6 \rightarrow C_8H_8 + 2H_2$	7.76×10^{15}	117.096
	8. Molecular Reaction II:		
132	$4C_6H_6 \rightarrow 3(C_4H)_X + 9H_2$	6.8×10^9	197.87
133	$4C_7H_8 \rightarrow 7(C_4H)_X + 12.5H_2$	6.8×10^9	203.16
134	$4C_8H_{10} \rightarrow 2(C_4H)_X + 4H_2$	6.8×10^9	212.05
135	$4C_8H_8 \rightarrow 2(C_4H)_X + 2H_2$	8.5×10^9	212.05
136	$2C_2H_6 \rightarrow C_3H_8 + CH_4$	1.2×10^{12}	233.32
137	$C_3H_6 + C_2H_6 \rightarrow C_4H_8 + CH_4$	1.18×10^{12}	259.19
138	$C_3H_8 \rightarrow C_2H_4 + CH_4$	4.69×10^{10}	178.28
139	$C_3H_8 \rightarrow C_3H_6 + H_2$	5.89×10^{10}	223.41
140	$2C_3H_8 \rightarrow 3C_2H_4$	1.2×10^{11}	263.98
141	$4C_2H_4 \rightarrow 2(C_4H)_X + 7H_2$	3.42×10^9	242.79

Table 6. Continued

Number	Reaction	Parameters adopted	
		A	E
142	$8C_3H_6 \rightarrow 3(C_4H)_X + 21H_2$	3.42×10^7	235.5
143	$C_4H_8 \rightarrow (C_4H)_X + 3H_2$	6.139×10^8	223.95
144	$C_4H_6 \rightarrow (C_4H)_X + 2H_2$	6.1408×10^8	242.3
145	$2C_2H_2 \rightarrow (C_4H)_X + H_2$	6.1408×10^8	242.3
147	$4C_{15}H_{34} \rightarrow 15(C_4H)_X + 60.5H_2$	1.0298×10^9	236.64
148	$C_{20}H_{28} \rightarrow 5(C_4H)_X + 11.5H_2$	6.139×10^8	205.04
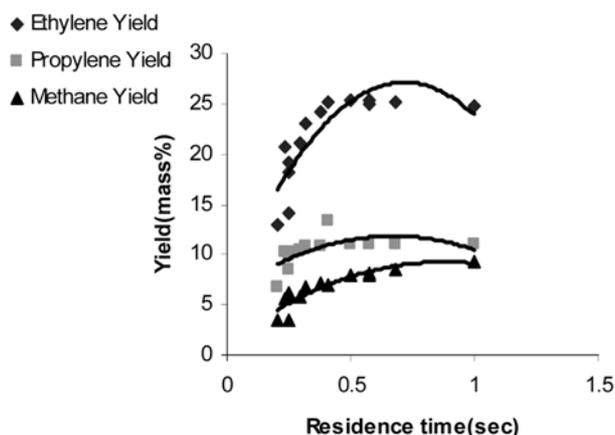
Fig. 2. Yield of ethylene, propylene and methane vs. residence time at steam ratio=1&COT=830 ºC.

Fig. 3. Yield of products vs. temperature. (a) At residence time= 0.4 sec, steam ratio=0.57. (b) At residence time=0.25 sec, steam ratio=0.888.

squares between the calculated concentration of the products and experimental values was used. It is used as an objective function and should be minimized.

In order to determine the rate constants of alkyl aromatic production reactions and the yield of these products, some analyses were carried out. Some experimental data on the yield of Benzene, Toluene, Ethylbenzene and Xylenes (BTEX) are shown in Table 5.

$(C_4H)_x$ which is a complex formula for coke represents the polymeric nature of the coke in Table 6.

RESULTS AND DISCUSSION

In addition to Table 4, several experiments were conducted in order to find out more about the dependency of the product yield distribution on operating parameters. Fig. 2 to Fig. 5 demonstrate the trends of yield of significant products vs. the variation of the operating variables. In fact, Fig. 2 demonstrates the dependency of yield of ethylene, propylene as the two main products and methane as by product, on the residence time.

This figure presents that increasing the residence time would increase the yield of ethylene and propylene, and these yields would have a downward trend after reaching the maximum point. However, the yield of methane increased without any changes in the trend.

The effects of the temperature on the yield of propylene, ethylene, butadiene and methane are demonstrated in Fig. 3.

Two different series of results reveal that increasing the temperature, at a constant residence time and steam ratio, would increase the yield of products.

By comparison between Fig. 3(a) and Fig. 3(b) the effect of the residence time is confirmed and the effect of steam ratio is shown as well. Concerning Table 6, ethylene and propylene are primary products, which are also contributed in the formation of the secondary products. By increasing the residence time and decreasing the steam ratio, more chances can be taken in order to progress the secondary reactions. This is due to assigning more time to the reactions and raising the concentration of reactants. This process would also lead to some differences in trends. In Fig. 3(b) the residence time is low and the steam ratio is high; therefore, the trends are steadily increasing. However, in Fig. 3(a) where the residence time is high and the steam ratio is low, the yields of ethylene and propylene are accordingly increasing. After reaching to a maximum point, propylene would have a sliding trend and the upward trend of ethylene yield becomes slow.
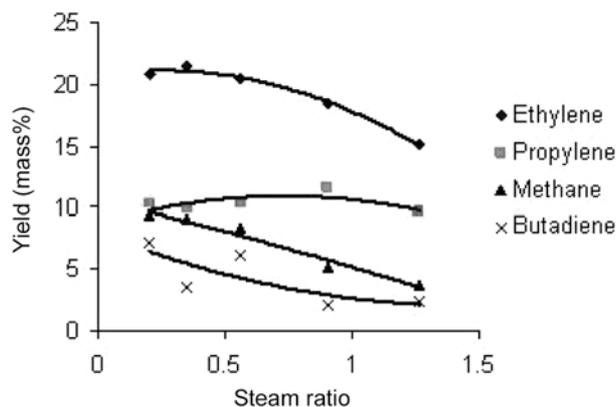
Fig. 4. Yield of products vs. steam ratio at residence time=0.4, COT =800 ℃.

Fig. 4 illustrates the results of experiments to study the effects of steam ratio on yield distribution of thermal cracking products.

As shown in this figure, the yield of ethylene and methane is continuously decreased by an increase in the steam ratio. However, in the range of experimental conditions, the trend of the yield of propylene has been changed.

Fig. 5 applies severity to describe the productivity of thermal cracking of atmospheric gasoil. The product yield distribution of thermal cracking of specific feedstock, in different reactors with different scales, is the same at a specific severity [16]. The severity used in this figure, is defined as follow:

$$S = COT * (Re \, sidence \, time)^{0.027} \tag{5}$$

As shown below, an increase in severity will increase the yield of different products. The maximum yield of products in the conducted experiments is obtained at the severity equal to 861.

The experimental results (Table 4) contain valuable concepts about thermal cracking of atmospheric gasoil. The maximum yield of obtained ethylene is 30.77% at COT; moreover, residence time and
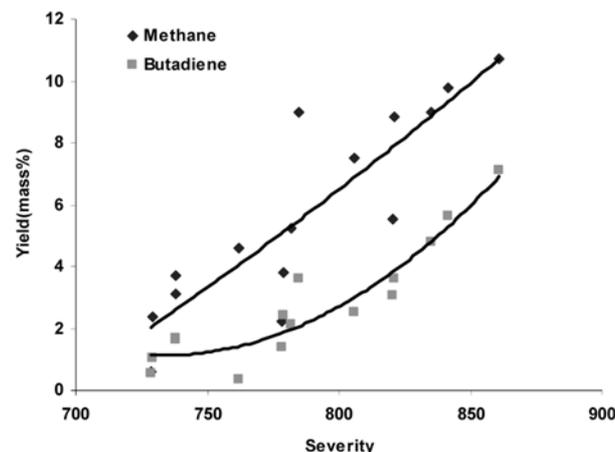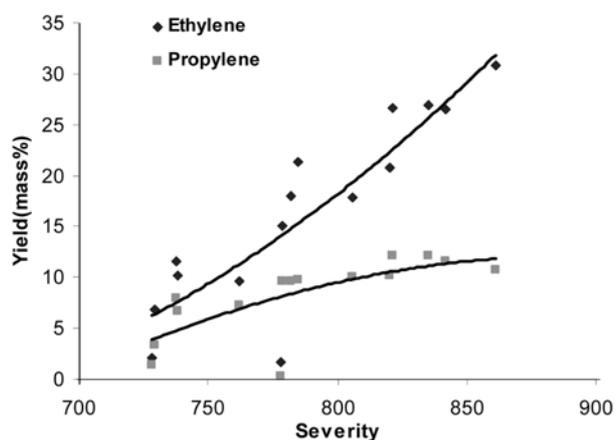
Fig. 5. Yields of products vs. severity.

steam ratio are equal to 885 ℃, 0.362 sec and 0.88, respectively. Nevertheless, the minimum is obtained at COT, residence time and steam ratio equal to 716 ℃, 0.36 sec and 0.8. The maximum yield of propylene is 12.2% and it is obtained at residence time, steam

Table 7. Comparison of the simulation and the experiment results

Parameter	Test 1		Test 2		Test 3		Test 4	
	Experiment	Model	Experiment	Model	Experiment	Model	Experiment	Model
COT (℃)	850	850	852	852	885	885	852.5	852.5
Feed flow rate (g/min)	2.334	2.334	4.958	4.958	3.253	3.253	2.052	2.052
Steam ratio	0.83	0.83	0.52	0.52	0.89	0.89	0.59	0.59
Yield (mass %)								
H_2	0.72	1.48	0.92	0.92	1.3	1.35	1.39	1.82
CH_4	9	8	8.83	7.51	10.72	8.77	9.81	9.12
C_2H_2	1.21	1.6	1.27	0.8	1.15	1.71	0.86	1.95
C_2H_4	26.94	25.69	26.66	24.72	30.77	28.96	26.52	27.3
C_2H_6	2.04	1.41	2.5	2.16	2.01	1.36	2.29	1.3
C_3H_6	12.22	10.7	12.21	11.65	10.72	10.57	11.62	10.36
C_3H_8	0.4	0.262	0.44	0.29	0.35	0.23	0.4	0.26
C_4H_6	5.56	6.19	3.18	4.75	7.28	9.46	5.65	7.26
C_4H_8	2.74	1.7	2.31	1.51	2.67	1.85	2.5	1.6
C5+	39.17	42.968	41.68	45.69	33.03	35.74	38.96	39.03

ratio and COT equal to 0.523 sec, 1.0 and 850 °C. The minimum is obtained at the same point at which the minimum yield of ethylene is obtained. The differences between the operating conditions of the maximum yields of ethylene and propylene are due to the contribution of these two main products in the secondary reactions. Maximum yield of propylene is obtained at a lower temperature in comparison with the temperature of the maximum yield of ethylene. In fact, this is due to the greater contribution of propylene in secondary reactions.

The ability to determine of the interactions of the different operating conditions effects on product yields is one of the advantages of conducting experiments based on the experimental design methods. An example of the interaction effects is illustrated by the results (No. 4 and 6 in Table 4). While the COT remained constant in these two experiments, the feed flow rate was varied from 2 g/min (code −1) for experiment no. 4 to 5 g/min (code 1) for experiment no. 6. In fact, the steam ratio changed from 1 (code 1) to 0.6 (code −1). Comparing between the yields of thermal cracking products for these two experiments proves almost the same results. However, the rate of coke formation has different trends. Experiment no. 6 shows lower rates of coke formation than experiment no. 4. This is due to the greater effects of residence time than the effects of steam ratio on rate of coke formation.

The developed model is used to determine the product yields dis-

tribution in the entire range of operating conditions. Table 7 demonstrates the results of experiments and the model at the same conditions. In fact, the results confirm the consistency of the developed model.

Fig. 6 and Fig. 7 present the product yields and the rate of coke formation which were generated by the model.

Fig. 6 shows the trends of the product yields and their convergence with experiments.

As Fig. 6 shows, the effects of steam ratio, temperature and residence time can be determined by the model as well as the experimental results. The trends of the yield of propylene and ethylene, (Fig. 3) are also provided in Fig. 6.

Fig. 7 demonstrates the trends of coke formation rate vs. COT. This figure shows that the coke formation rate has a steady upward trend vs. COT. In fact, it is slow at the lower COT and rises faster when the COT increases. This trend is dependent on the reactions, which form the coke. These secondary reactions start to proceed after the primary products begin to form. Comparing Fig. 7(a) and 7(b), it shows that low residence time and high steam ratio decrease the rate of coke formation.

The main product yields vs. the length of the reactor are shown in Fig. 8. In general, the yields of thermally stable products such as methane and aromatic components increase continuously along the
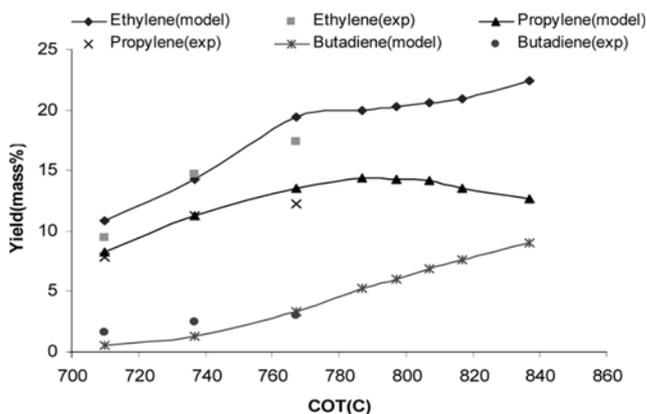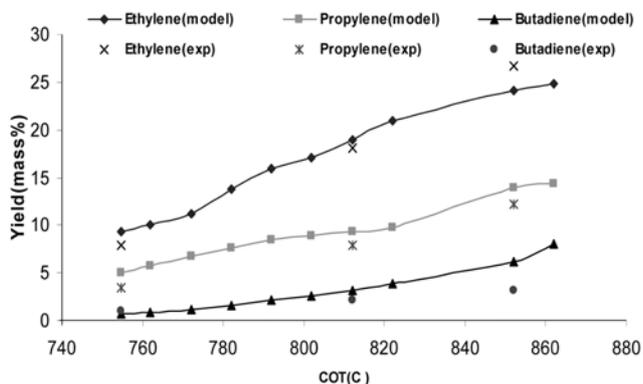

Fig. 6. Yields of products generated by the model vs. COT (°C). (a) At Residence time=0.538 sec and steam ratio=0.647 (b) at residence time=0.257 sec and Steam ratio=0.522.
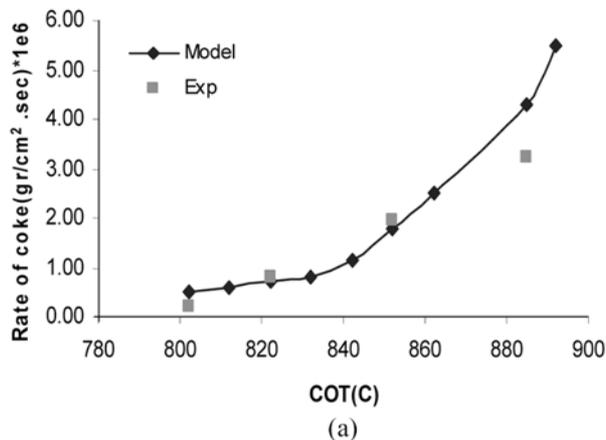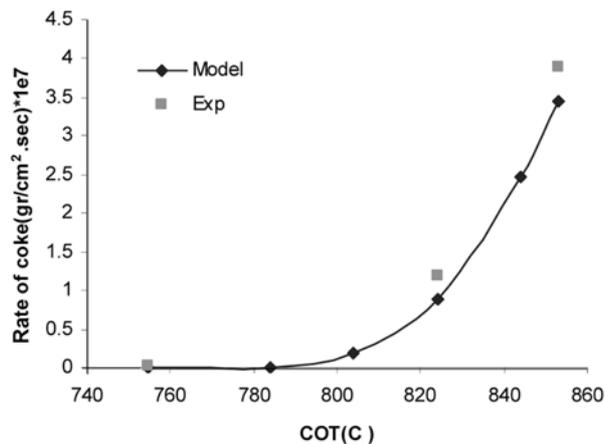
Fig. 7. Coke formation rates predicted by developed model vs. COT (°C). (a) residence time=0.362 sec steam ratio=0.88 (b) residence time=0.24 sec, steam ratio=1.0523.
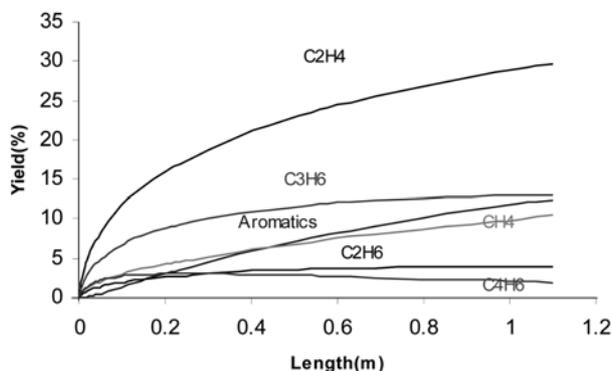
Fig. 8. Profile of yields of main products along the reactor at residence time=0.6 sec, COT=845 ℃, steam ratio=0.5.
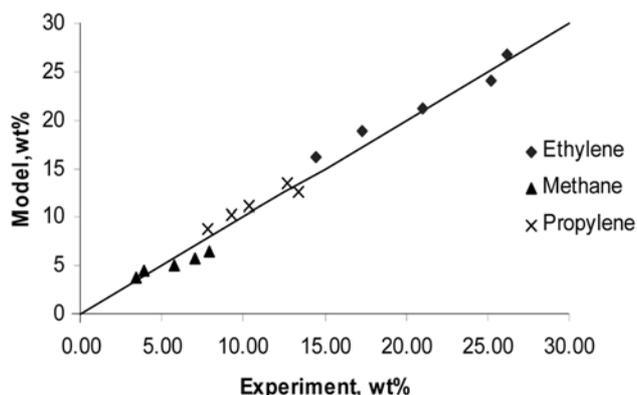

Fig. 9. Scatter diagram of ethylene, methane and propylene yield.

reactor. The yield of butadiene increases and reaches the maximum value and then decreases.

The residual deviation between measured and calculated yields of ethylene, methane and propylene are presented in Fig. 9. The scatter diagram shows the overall favorable agreement between the predicted and the experimental data.

CONCLUSIONS

Thermal cracking of atmospheric gasoil was studied by conducting several experiments. First, in order to characterize the atmospheric gasoil, some experiments and calculations were carried out. The results show that this is a paraffinic feedstock with 32% normal paraffins, 22% iso paraffins, 30% naphthenes, 11.7% alkyl aromatics and 2.8% poly aromatics. In addition, the experiment shows that atmospheric gasoil has coking inhibition index equal to 36.75. The results prove the suitability of this atmospheric gasoil for being a feed stock of thermal cracking. Next, several thermal cracking experiments were conducted in a pilot plant. The results demonstrate that increasing temperature and residence time would consequently increase the rates of primary and secondary reactions. However, an increase in steam ratio would decrease the yield of secondary products. Furthermore, the specific trends of ethylene and propylene revealed their contributions in the formation of secondary products.

In order to apply the experimental results to other reactors with

different scales, the severity is utilized. It is confirmed that the yields of different products have decreasing trends with increasing the severity. The maximum yields of products were at severity equal to 861.

Nineteen tests of the total conducted experiments were designed by CCD method. Regarding the results, the yield of ethylene and propylene can respectively reach to 30% and 12.2%.

Based on these experiments a kinetic model has been modified. In addition to the previous model for thermal cracking of atmospheric gasoil, both the production of acetylene and the contribution of all olefins, acetylene, aromatics and poly aromatics in coke formation have been concerned in this model. The trends of main products and rate of coke formation are studied by the modified model. The modeling results reveal that increasing the COT and residence time would increase the rate of coke formation as a secondary product. However, raising the steam ratio decreases it.

ACKNOWLEDGMENTS

NOMENCLATURE

a : conversion factor
A : frequency factor [1/sec] or [L mol^{-1}sec^{-1}]
COT : coil outlet temperature [℃]
C_{Pj} : specific heat capacity of jth component [Joul/mol K]
d_t : diameter of reactor tube [m]
E : activation energy [kJoul/mol]
F_j : molar flow rate of jth component [mol/sec]
Fr : friction factor [--]
G : total mass flux of the process gas [kg/m^2·sec]
M_m : molecular weight of mixture [g/mol]
P : pressure [kPa]
Q : heat flux [kW/m^3]
r_{ri} : rate of reactions [mol/m^3·sec]
R : universal gas constant [kPa*m^3/mol*K]
Re : Reynolds number [--]
S : severity [℃*sec$^{0.027}$]
S_{ij} : stoichiometric factor
T : temperature [K]
X_1 : experimental design factor, hydrocarbon feed flow rate [g/min]
X_2 : experimental design factor, steam ratio [--]
X_3 : experimental design factor, coil outlet temperature [℃]

REFERENCES

1. A. Niaei, J. Towfighi, S. M. Sadreameli and R. Karimzadeh, *Applied Thermal Engineering*, **24**, 2251 (2004).
2. S. M. Sadreameli and A. E. S. Green, *Journal of Analytical and Applied Pyrolysis*, **73**, 305 (2005).
3. M. E. Masoumi, S. M. Sadreameli, J. Towfighi and A. Niaei, *Energy*, **31**, 516 (2006).
4. K. Y. Grace Chan, F. Inal and S. Senkan, *I & EC Research*, **37** (1998).
5. H. Manafzadeh, S. M. Sadreameli and J. Towfighi, *Applied Ther-*

mal Engineering, **23**, 1347 (2003).

6. S. B. Zdonik, G. L. Hayward and S. H. Fishtine, *Hydrocarbon processing*, December (1975).

7. V. Kaiser, D. Gilbourne and C. A. Pocini, *Hydrocarbon processing*, April (1977).

8. M. Hirato, S. Yoshioka and Matanuska, *Hitachi Rev.*, **20**(8), 326 (1971).

9. M. Hirato and S. Yoshioka, *International Chemical Engineering*, **13**(2), 347 (1973).

10. D. Depeyre, C. Flicoteaus, F. Arabzadeh and A. Zabaniotou, *I& Eng. Chem. Res.*, **28**(7) (1989).

11. P. J. Clymans, G. F. Froment, M. Berthelin and P. Trambouze, *AIChE J.*, **30**(6), 904 (1988).

12. E. Ranzi, T. Faravelli, P. Gaffuri, E. Garavaglia and A. Goldaniga, *Ind. Eng. Chem. Res.*, **36**, 3336 (1997).

13. E. Ranzi, M. Dente, A. Goldaniga, G. Bozzano and T. Faravelli, *Progress in Energy and Combustion Science*, **27**, 99 (2001).

14. J. E. Gwyn, *Fuel Processing Technology*, **70**, 1 (2001).

15. F. Shubo, S. Liming and L. Qiangkun, *Journal of Analytical and Applied Pyrolysis*, **65**, 301 (2002).

16. L. F. Albright, B. L. Crynes and W. H. Corcoran, *Pyrolysis: Theory and industrial practice*, Academic Press (1983).

17. M. Dente, E. Ranzi, G. Bozzano, T. Faravelli and P. J. M. Valkenburg, *Heavy component description in the kinetic modeling of hydrocarbon pyrolysis*, AIChE Spring National Meeting, April 23 (2001).

18. U. Taskar and J. B. Riggs, *AIChE J.*, **43**(3), 740 (1997).

19. S. Zahedi. Abghari, S. S. Mohaddecy, S. Sedighi and H. Bonyad, Proceeding of 10th Iranian chemical engineering conference, 3372 (2005).

20. M. R. Riazi and T. E. Daubert, *Hydrocarbon processing*, 115 (March 1980).

21. J. Towfighi, A. Niaei, R. Karimzadeh and G. Saedi, *Korean J. Chem. Eng.*, **23**, 816 (2006).

22. K. M. Sundaram and G. F. Froment, *Chemical Engineering Science*, **32**, 601 (1977).

23. R. Zou, *Fundamentals of pyrolysis in petrochemistry and technology*, Lewis Pub (1993).

24. G. E. P. Box and N. R. Draper, *Empirical model-building and response surfaces*, John Wiley & Sons (1987).

25. C. F. Gerold and P. O. Wheatley, *Applied numerical analysis*, Addison-Wesley publishing company (1984).